Recent origin of Saturn's moonlets and F-ring from rings viscous spreading

Sébastien CHARNOZ[*]
Equipe AIM, Université Paris Diderot /CEA/CNRS
91191 Gif sur Yvette Cedex FRANCE

Julien SALMON
Equipe AIM, Université Paris Diderot /CEA/CNRS
91191 Gif sur Yvette Cedex FRANCE

Aurélien CRIDA
Department of Applied Mathematics and Theoretical Physics,
University of Cambridge, UK.
Laboratoire Cassiopée, Université de Nice Sophia-Antipolis/CNRS/Observatoire de la Côte d'Azur, BP4229, 06304 Nice Cedex 4, FRANCE.

(*) To whom correspondence should be addressed (charnoz@cea.fr)

The regular satellites of the giant planets are believed to have finished their accretion concurrent with the planets at about 4.5 Gy ago [1,2,3,4]. A population of Saturn's small moons, that orbit just exterior to the main rings, challenges this conception because they are dynamically young[5,6] (less than 10^7 years). They are also under-dense[7] (~600 kg/m^3) and show spectral characteristics similar to the rings[8,9]. Some authors have suggested they might have accreted at the rings' edge[7,10,11]. However their formation and coupled evolution with the rings was never simulated because of the too-short orbital timescales, casting doubts on this hypothesis. Using a hybrid simulation we unveil a mechanism by which the viscous spreading of Saturn's rings beyond the Roche Limit (the distance beyond which the rings are gravitationally unstable) gives birth to the today's small-moons: masses distribution and orbital architecture are reproduced. The current confinement of the main rings and the presence of the dusty F-ring are shown to be direct consequences of this mechanism that couples viscous evolution and satellite formation. Saturn's rings, like a mini-protoplanetary disk, may be the last place where accretion was recently active in the Solar System, some 10^6 to 10^7 years ago.

The low density of Saturn's small moons, their icy composition, closeness to the rings and rapid tidal timescales have suggested for long that a genetic link may exist with Saturn's icy rings. On the one hand, the population of small moons exterior to the Roche Limit (Atlas, Prometheus, Pandora, Janus and Epimetheus) have a mass/distance relation remarkably different from Saturn's main satellites (Fig. 1). On the other hand, N-body simulations[10,12] show that ring material spreading viscously beyond 142,000 km would be gravitationally unstable and that ~100 m aggregates would form in less than 10 orbits. Below 138,000 km, accretion becomes inefficient[12,13,14], so the outer edge of the region where accretion is prevented (the "Roche Region") is $R_L \approx 140000 \pm 2000$km. R_L differs slightly from the classical definition of the Roche Limit since its precise location depends on a diversity of factors like the bodies' relative size, spin[14,15] etc. Today, the ring's outer edge is sharply confined at 136,775 km by Janus' gravitational torque[5,16]. However this configuration must be transient (<10 My) because the rings repel Janus and, in turn, the ring is pushed inward to conserve angular momentum. As the moon migrates outward, the rings' edge confinement location moves accordingly and may pass the nearby Roche Limit. So ring material may have spread across Saturn's Roche Limit in the past, or will do in the future.

To simulate on long-timescales (~10^9 years) the coupled evolution of aggregates with the rings we designed a hybrid model in which two codes are self-consistently coupled[17]: (1) a 1D-hydrodynamical model to track the ring's viscous evolution and (2) an analytical orbital model to track the moonlets. The evolution of the ring's surface density $\sigma(r)$ is computed using a finite-element scheme, on a staggered mesh, solving for the surface-density equation of a keplerian disk under the effect of viscous torque and moonlets' gravitational-torques [18]:

$$\frac{d\sigma}{dt} = \frac{3}{r}\frac{\partial}{\partial r}\left[r^{1/2}\frac{\partial}{\partial r}\left(\nu(r)\sigma r^{1/2}\right) - \frac{1}{3\pi\sqrt{GM}} r^{1/2} T(r) \right], \quad \textbf{Eq. 1}$$

where r, $\nu(r)$, G and M are the distance, local viscosity, gravitational constant, and Saturn's mass respectively. T(r) is the sum, for all the satellites, of the Lindblad resonances torque densities located at distance r from Saturn (Supplementary Information, section 1). A realistic viscosity model, which is an increasing function of the surface density, is implemented[19]. Because aggregates are formed at $r \geq R_L$ after only a few orbital periods (negligible compared to viscous timescales), the accretion of ring material into moonlets is considered to occur instantaneously: at each time step, all ring mass located beyond R_L is removed from the hydrodynamical simulation and transformed into one additional satellite.

Every individual satellite is tracked and its mass m_s, semi-major axis a_s and eccentricity e_s are tabulated (SI, section 2). The resultant eccentricities are so small ($<10^{-4}$) that they do not influence the system's evolution. The semi-major axes evolve under the effects of planet's tides and ring torque according to:

$$\frac{da_s}{dt} = \frac{3k_{2\mathrm{p}} m_s G^{1/2} R_p^5}{Q_p M^{1/2} a_s^{11/2}} + \frac{2a_s^{1/2}\Gamma_s}{m_s (GM)^{1/2}} \quad \textbf{Eq.2}$$

where Q_p, k_{2p}, R_p stand for the planet's dissipation factor, Love number, and radius respectively (SI, section 1.2). Γ_s is the sum of the ring torques for all first-order Lindblad resonances of the satellite [6,18,20]. When the orbital separation of two satellites is smaller than 2.2 mutual Hill radii, they are merged[12]. To test the full procedure, the Moon formation from a circumterrestrial disk was successfully reproduced[21] (SI, section 3).

The initial conditions are as follows : the A ring is initially represented by a disk extending from 122,000 km to 136,000km with a constant surface density σ_0. The initial state of Saturn's rings is unknown and they could have been denser in the past[22]. Cases with σ_0=400, 1000, 5000 and 10^4 kg/m^2 have been considered. The case with σ_0=400 kg/m^2 is presented (about the present surface density of Saturn's A ring. Fig. 2). R_L is set to 140000 km.

The simulation starts with no satellite so that the ring spreads freely initially and reaches R_L in ~10^6 years (Fig. 2). Then, moonlets accrete at R_L from the ring material and grow through mutual encounters. They induce step-like structures in the ring's surface density near moonlets' Lindblad resonances (Fig 2.a-d). At these locations the ring angular-momentum is directly transferred to the satellites, inducing an orbital decay of the ring material and an expansion of the satellites' orbit. As a consequence, the ring material moves inward and accumulates just interior to the resonant location, resulting in the visible step-like structures in the surface-density function. While Γ_s increases with the moonlet's mass, the disk's surface density decreases due to spreading and thus so do the viscosity and the viscous torque (Γ_v) [16]. When the magnitude of Γ_s becomes larger than that of Γ_v, the disk's outer edge is confined and the disk stops spreading (Fig.2.e). This happens when the largest moon reaches ~10^{17} kg (and ~10^{18} kg) for $\sigma_0 \leq 1000$ kg/m^2 (and $\sigma_0 \geq 5\times10^3$ kg/m^2). As the moonlets' masses increase, the ring's outer edge shifts inward down to the position of the first Lindblad resonance for which the torque is strong enough to counterbalance Γ_v. On long timescales, due to the decrease of the surface density, confinement is increasingly easier and, in this model, the outer edge is around ~135,000 km at 4×10^9 yrs for $\sigma_0=400$ kg/m^2. For higher values of σ_0, the disk spreads viscously more rapidly, more massive moonlets are formed; this ultimately shifts the disk's edge even below 130,000km. In conclusion, the current confinement of Saturn's rings outer edge seems the consequence of on-going satellite accretion occurring at the Roche Limit. The outer-edge jumps from one resonance to another, depending on the local balance between the positive viscous torque and negative torque induced by the population of small moons.

Concerning the moonlets, they migrate outward due to the positive induced by the rings and the planet. Since both torques are increasing functions of the satellite's mass[20] ($\Gamma_s \propto m_s^2$) their migration rate increases accordingly and more massive satellites migrate more rapidly. Different migration rates lead to crossings and merging. Since all satellites appear at the same location (R_L) a simple orbital architecture appears in which satellites are radially sorted: their distance to Saturn is an increasing function of their mass, in agreement with observations (Fig. 1). So the actual orbital architecture of the small moons may be the direct consequence of ring/satellites interactions.

These results imply also that Saturn's small moons are gravitational aggregates made of icy ring particles which would explain naturally their very low densities. When they form, they should be initially elongated like Hill spheres [7,10] like observed for some of the moons[7] . Pandora or Epimetheus seem to deviate somewhat from this shape[7], but this could result from post-accretional restructuration. The moons' spectral similarities with Saturn's rings [9,24] may be the direct result of their formation within the rings, as well as their apparent absence of silicates[7] since Saturn's rings seem devoid of such material [8,24].

The coupling of the ring-confinement with moonlet's migration induces a feedback on the formation rate of the moonlets. When the ring's edge is repelled below R_L, the moonlet production stops (compare Fig. 2.e and 2.f). Conversely, as satellites recede away, the location of the ring's edge follows and satellite production can set-in again for any ring material that reaches R_L. This stop-and-go mechanism is apparent in the mass history of satellites (Fig. 2.f): it limits their mass to about the smallest mass necessary to confine the ring and can be analytically estimated (SI, section 4). The mass-distributions of moonlets obtained in our simulations matches well the observed one with similar cumulative indexes and overall shape (Fig. 3). However, these results may be affected by non-linearities that could appear in the torque of the most massive satellites (SI, section 3.4). A direct consequence of this feedback mechanism is that the mass of the largest moon must be of the order of the mass necessary to confine the ring: this is actually the case with Janus, the most massive of the small moons, that confines the A ring's outer edge[5,16]. The current mass of Janus implies that the A ring surface density was between 10^3 kg/m^2 and 5×10^3 kg/m^2 at the time Janus formed (whereas the ring's total mass remains undetermined[23]).

Saturn's main rings are encircled by a dusty and dynamically active ringlet, called F-ring, located at 140,500 km, whose origin is still debated. In the present work, its presence may have a simple explanation: due to the spreading of the A ring, aggregates are formed around 140,000 km and suffer subsequent collisional evolution while migrating outward. Since accretion should not be 100% efficient below 142,000km[14] colliding aggregates will release dust and produce a dusty ring with a non-negligible mass, like today's F-ring [25,26,27] . In the current orbital configuration, the F ring is not feed with new aggregates coming from the A ring because of the confinement induced by Janus. However, on longer timescales, the dusty F ring will be fed again when the A ring viscously spreads again. Thus, the F ring would have been always present because of the regular renewing of its material. In this scenario, it is envisioned as the dusty signature of ring material crossing the Roche Limit due to the global viscous spreading of the rings. The age of the F-ring material would be about the same as the nearby moonlets[25], 10^{6-7} years, even though the main rings could be older.

REFERENCES

1. Mosqueira I., Estrada P.R. Formation of the regular satellites of giant planets in an extended gaseous nebula I: subnebula model and accretion of satellites. *Icarus* **163**, 198-231 (2003)

2. Canup, R., and Ward, W. R. Formation of the Galilean satellites: Conditions for accretion. *Astron. J.* **124**, 3404-3423 (2002)

3. Canup R.M., Ward W.R. A common mass scaling for satellite systems of gaseous planets. *Nature* **411**, 834-839 (2006)

4. Estrada, P. R., Mosqueira, I., Lissauer, J. J., D'Angelo, G., and Cruikshank, D. P. Formation of Jupiter and conditions for the accretion of the Galilean satellites. To appear in: Europa (McKinnon, W., Pappalardo, R., Khurana, K., eds.), University of Arizona Press, Tucson (2010)

5. Lissauer J.J., Cuzzi J.N. Resonances in Saturn's rings. *Astron. J.* **87**, 1051-1058 (1982)

6. Poulet F., Sicardy B. Dynamical evolution of the Prometheus-Pandora system. *MNRAS* **322**, 343-355 (2001)

7. Porco C.C., Thomas P.C., Weiss J.W., Richardson D.C. Physical characteristics of Saturn's small satellites provide clues to their origins. *Science* **318**, 1602-1607. (2007)

8. Poulet F., Cruikshank D.P., Cuzzi J.N., Roush T.L., French R.G. Compositions of Saturn's rings A, B, and C from high resolution near-infrared spectroscopic observations. *A&A* **412**, 305-316 (2003)

9. Coradini A,; Capaccioni F., Cerroni P., Filacchione G., Magni G., Orosei R., Tosi F., Turrini D. Saturn Satellites as Seen by Cassini Mission. *EM&P* **105**, 289-310 (2009)

10. Karjalainen R., Salo H. Gravitational accretion of particles in Saturn's rings. *Icarus* **172**, 328-348 (2004)

11. Charnoz S., Brahic A., Thomas P., Porco C. The equatorial ridges of Pan and Atlas: Late accretionary ornaments? *Science* **318**, 1622-1624 (2007)

12. Karjalainen R. Aggregate impacts in Saturn's rings. *Icarus* **189**, 523-537 (2007)

13. Ohtsuki K. Capture probability of colliding planetesimals: Dynamical constraints on accretion of planets, satellites, and ring particles. *Icarus* **106**, 228–246 (1993)

14. Canup, R. M., Esposito, L. W. Accretion in the Roche zone: Coexistence of rings and ring moons. *Icarus* **113**, 331-352 (1995)

15. Weidenschilling S.J., Chapman C.R., Davis D.R., Greenberg R. Ring particles: collisional interactions and physical nature. In *Planetary Rings* (R. Greenberg and A. Brahic *Eds.*), pp 367-415. univ. of Arizona Press, Tucson (1984)

16. Spitale J.N., Porco C.C. Time variability in the outer edge of Saturn's A-Ring Revealed by Cassini imaging. *Astron. J.* **138**, 1520-1528 (2009)

17. Salmon J., Charnoz S., Crida A. Long-term and large scale simulation of Saturn's rings viscous evolution. To appear in *Icarus* (2010)

18. Takeuchi T., Miyama S.M., Lin D.N.C. Gap formation in protoplanetary disks. *ApJ* **460**, 832-847 (1996)

19. Daisaka H., Tanaka H., Ida S. Viscosity in a Dense Planetary Ring with Self-Gravitating Particles. *Icarus* **154**, 296-312 (2001)

20. Meyer-Vernet N., Sicardy B. On the physics of resonant disk-satellite interaction. *Icarus* **69**, 157-175 (1987)

21. Kokubo E., Ida S., 2000. Makino J. Evolution of a circumterrestrial disk and formation of a single moon. *Icarus* **148**, 419-436 (2000)

22. Charnoz S., Morbidelli A., Dones J., Salmon A. Did Saturn's rings form during the Late Heavy Bombardment ? *Icarus* **199**, 413-428 (2009)

23. Charnoz, S., L. Dones, L. W. Esposito, P. R. Estrada, M. M. Hedman, in *Saturn from Cassini-Huygens*, M. K. Dougherty, L. W. Esposito, T. Krimigis, Eds. (Springer Netherlands), pp. 535-573 (2009)

24. Cuzzi J., Clark R., Filacchione G., French R., Johnson R., Marouf E., Spilker L. Ring particle composition and size distribution, in *Saturn from Cassini-Huygens*, M. K. Dougherty, L. W. Esposito, T. Krimigis, Eds. (Springer Netherlands), pp. 535-573. (2009)

25. Murray C.D., Beurle K., Cooper N.J., Evans M.W., Williams G.A., Charnoz S. The determination of the structure of Saturn's F ring by nearby moonlets. *Nature* **453**, 739-744 (2008)

26. Showalter M.R., Pollack J.B., Ockert M.B., Doyle L.R.,Dalton J.B. A photometric study of Saturn's F ring. *Icarus* **100**, 394-411 (1992)

27. Charnoz S. Physical collisions of moonlets and clumps with the Saturn’s F ring core. *Icarus* **201**, 191-197 (2009)

ACKNOWLEDGEMENTS

This work was funded by Université Paris Diderot and CEA/IRFU/SAp. S. Charnoz, J. Salmon and A. Crida designed the code and led the scientific investigation presented here. The authors thank F. Bournaud, J. Burns, L. Dones, Z. Leinhardt, H. Throop. Reprints and permissions information is available at npg.nature.com/reprintsandpermissions . The authors declare no competing financial interests. Correspondence and requests for materials should be addressed to charnoz@cea.fr.

LEGENDS OF FIGURES

Figure 1: Mass of Saturn's inner moons versus distance. Their names and average diameters are indicated in thumbnails images. Mimas, Enceladus and Tethys are also plotted for comparison. The vertical dashed line shows the location of the outer edge of Saturn's A ring at 136,750km, the vertical dashed-dotted lines stands for the F-ring location (a ~1000 km wide ringlet located between Prometheus and Pandora). Blue and red thick lines show simple log-fits to the mass/distance relations for small moons and main moons, respectively. Images credit: Cassini (NASA/JPL/SSI).

Figure 2: The time evolution of a model with σ_0=400 Kg/m^2. (a) to (d): the time evolution of the ring's surface density (solid line, left scale) and the satellite system as a function of distance (black circles, right scale). As the ring spreads inward and outward, its surface density decreases. Ring material crossing the Roche Limit (R_L=140000 km here) is transformed into moonlets. At the end of the simulation only 1.5×10^{18} kg of material remains in the A ring whereas 3.5×10^{18} kg spread below 120,000 Km and 1.8×10^{17} kg were transformed into moonlets; (e) The time evolution of the location of the ring's outer edge, defined as the place where the surface density drops below 1kg/m^2. When the edge is confined at the location of a satellite's resonance, the disk's viscous torque (that tends to push material beyond the ring's edge by transferring angular momentum) is perfectly balanced by the satellite's gravitational torque, thus the ring material is prevented from spreading further outward; (f) solid line: total mass into satellites as a function of time; dashed line: mass of the largest satellite.

Figure 3: Comparing the mass-distribution of the moonlets obtained in our simulation with observations. The cumulative mass-distributions of moonlets obtained in four simulations with different initial surface-densities (σ_0) are fitted with single power-law functions N(>m)$\propto$ $m^{-\alpha}$: Case A (green) : σ_0 = 400 kg/m^2 (α=0.31±0.06); Case B (yellow): σ_0 = 1000 kg/m^2 (α=0.19±0.01); Case C (red): σ_0 = 5000 kg/m^2 (α=0.22±0.03); Case D (blue): σ_0 = 10000 kg/m^2 (α=0.17±0.04). The actual population of Saturn's moonlets (black solid line, with label Sat., α=0.27±0.07) is well in the range of masses and number of bodies obtained in the simulations. Note that some of our distributions (A,B and C) show a knee and a shallower slope at smaller sizes, as observed for Saturn's small moons.

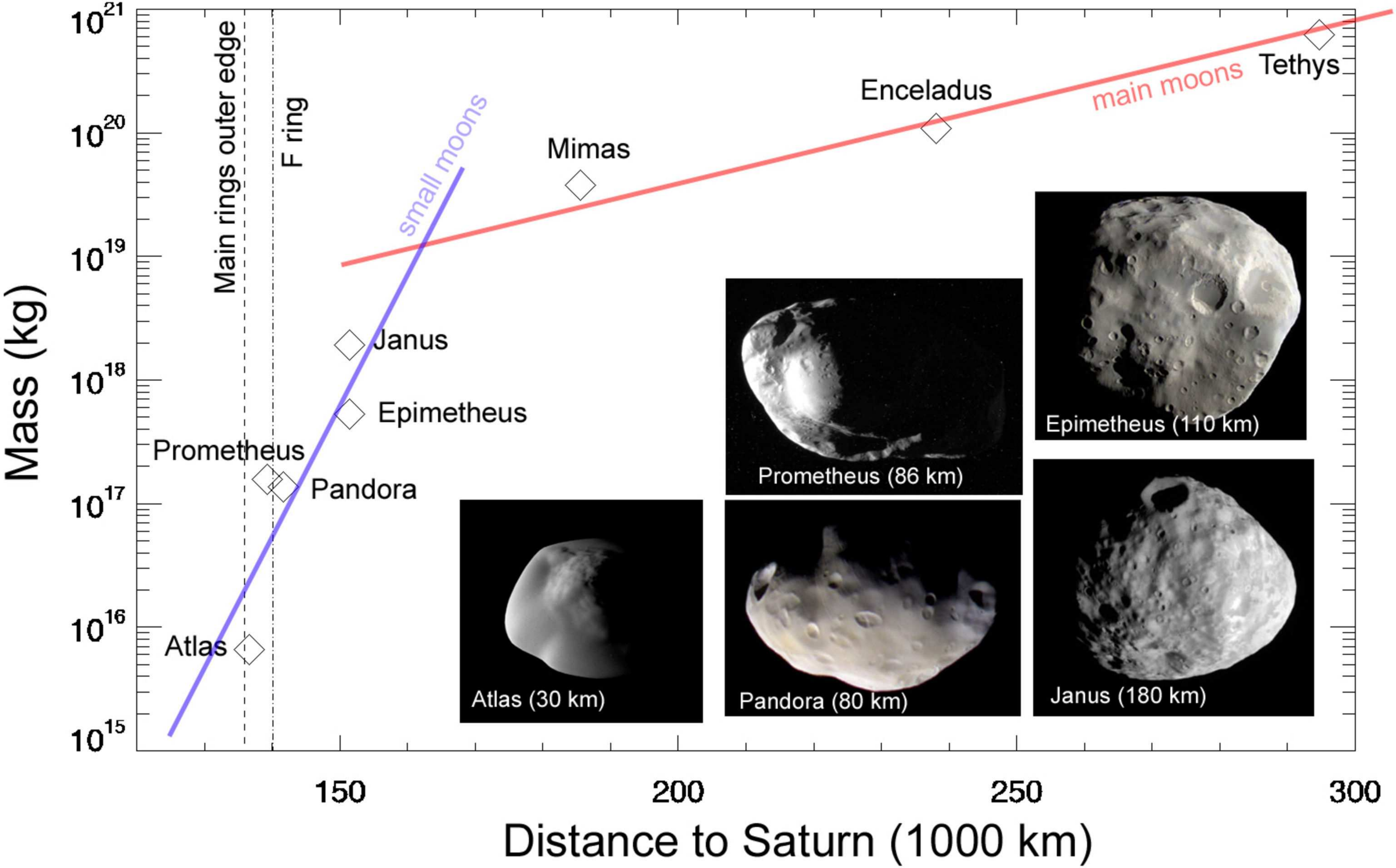

Mass (kg)
10^{21}
10^{20}
10^{19}
10^{18}
10^{17}
10^{16}
10^{15}
Main rings outer edge
F ring
small moons
main moons
Mimas
Enceladus
Tethys
Janus
Epimetheus
Prometheus
Pandora
Atlas
Atlas (30 km)
Pandora (80 km)
Prometheus (86 km)
Epimetheus (110 km)
Janus (180 km)
150
200
250
300
Distance to Saturn (1000 km)

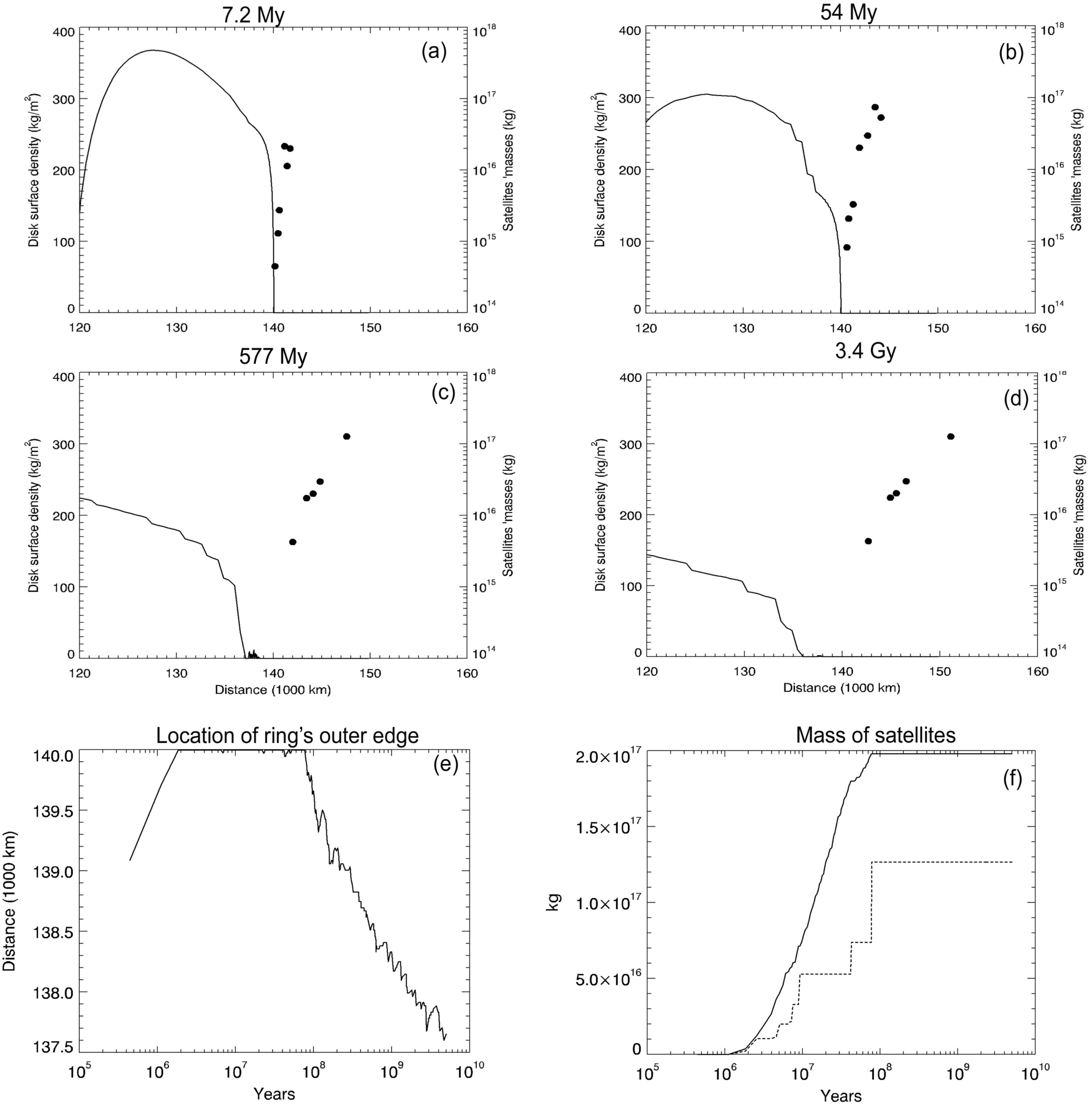
7.2 My
(a)
54 My
(b)
577 My
(c)
3.4 Gy
(d)
Disk surface density (kg/m^2)
Satellites 'masses (kg)
Distance (1000 km)
0
100
200
300
400
10^{14}
10^{15}
10^{16}
10^{17}
10^{18}
120
130
140
150
160
Location of ring's outer edge
(e)
Distance (1000 km)
137.5
138.0
138.5
139.0
139.5
140.0
Years
10^5
10^6
10^7
10^8
10^9
10^{10}
Mass of satellites
(f)
kg
0
5.0×10^{16}
1.0×10^{17}
1.5×10^{17}
2.0×10^{17}
Years

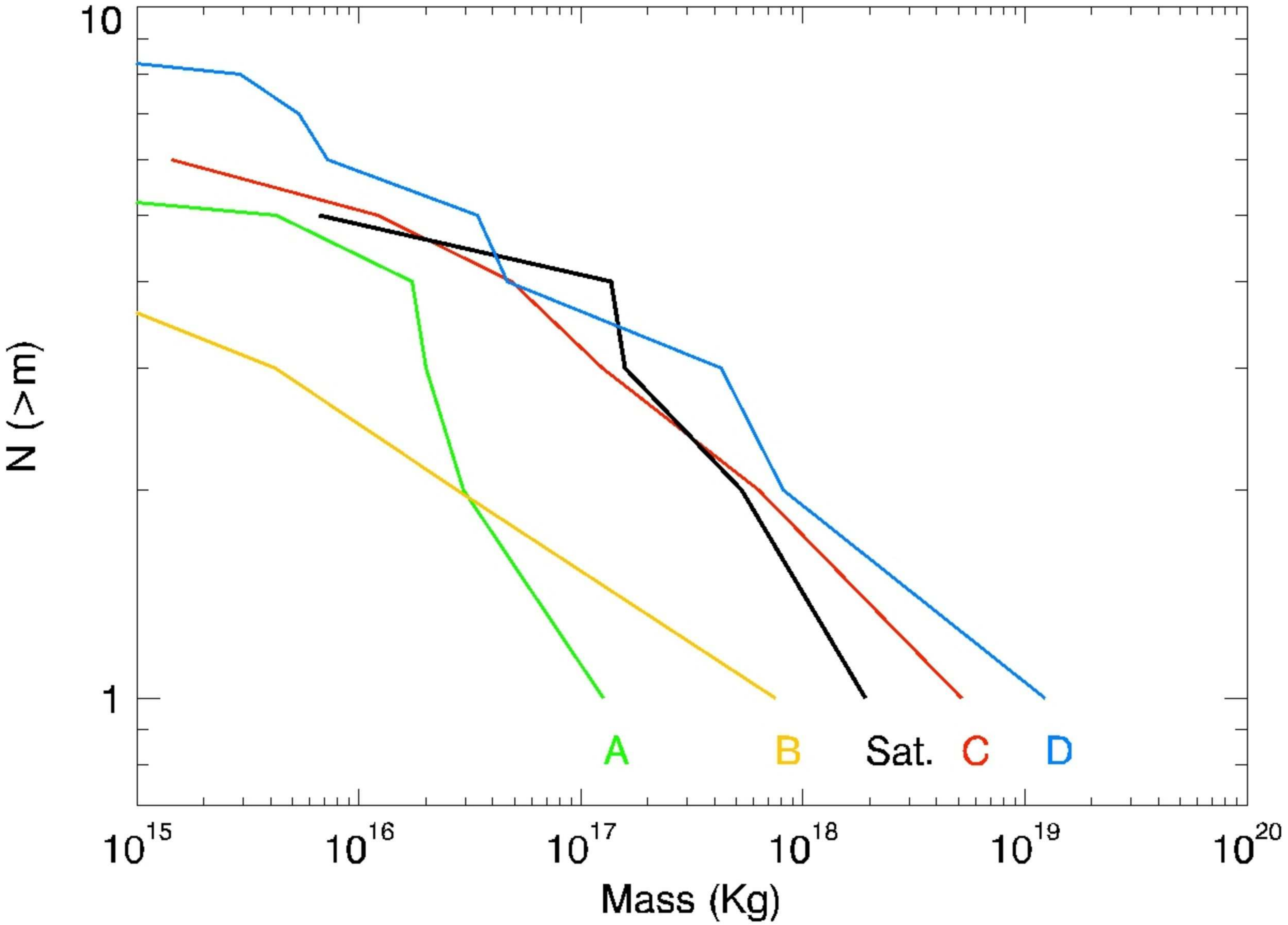
N (>m)
10
1
Mass (Kg)
10^{15}
10^{16}
10^{17}
10^{18}
10^{19}
10^{20}
A
B
Sat.
C
D